



## A Graphene Based Broadband Metasurface Absorber in the Terahertz Region

Sambit Kumar Ghosh<sup>(1)</sup>, Santanu Das<sup>(2)</sup>, and Somak Bhattacharyya\*<sup>(3)</sup>

(1), (3) Department of Electronics Engineering, Indian Institute of Technology (BHU), U.P.-221005, India

(2) Department of Ceramic Engineering, Indian Institute of Technology (BHU), U.P.-221005, India

### Abstract

This article proposes the design of a graphene-based metasurface that can have a wide absorption bandwidth in the terahertz region. The unit segment of the proposed structure is composed of three parts stacked to each other. A graphene-based plus-shaped pattern is deposited on the top of an amorphous silicon dioxide ( $\text{SiO}_2$ ) dielectric substrate layer. Another square-shaped graphene pattern covers the backside of  $\text{SiO}_2$  completely. The top graphene geometry is an optimized one, which can achieve a wide absorption bandwidth of more than 90% absorptivity over a bandwidth of 12 THz ranging from 7 THz to 19 THz. The proposed metasurface achieves two closed absorption peaks at 9.55 THz and 12.5 within the above said spectral range. The design is ultrathin in nature and it is in the order of  $\lambda/30$ . The periodicity of the structure is approximately  $\lambda/7.5$ . The designed prototype is polarization independent in nature. This particular graphene-based metasurface works well upto 60° of the incident angles of the incoming electromagnetic wave to the top surface of the structure under both TE and TM polarizations.

### 1. Introduction

Metasurface has been evolved as a tree, which has several fruitful branches of applications in different fields of science viz., antenna, modulators, filters, phase shifters, cloaking devices, polarizers etc [1-5]. Till date, different types of compact and ultra-thin metasurface absorbers have been presented in several literatures for single band, dual band and multi-band applications in the microwave, millimetre wave/sub-millimetre wave regions along with the terahertz region [6-8]. Single layer as well as multi-layered thick graphene-based absorbers with less bandwidth have also been designed in some of the previous literatures in the terahertz regime but they are difficult to fabricate in reality [9].

A graphene-based metasurface is presented in this article whose unit cell contains three layers. One amorphous silicon dioxide ( $\text{SiO}_2$ ) block is inserted between two different graphene patterns in the proposed unit cell where the top surface contains plus-shaped graphene pattern while the bottom surface is completely graphene backed. The designed prototype is optimized in such a way that it can exhibit more than 90% absorptivity over a large absorption bandwidth from 7 THz to 19 THz with two

closed absorption peaks at 9.55 THz and 12.50 respectively. The structure is independent of polarization of the EM wave approaching to the top layer of the designed metasurface. In addition, it works well upto 60° of the incident angles under both TE and TM polarizations.

### 2. Design of the Structure

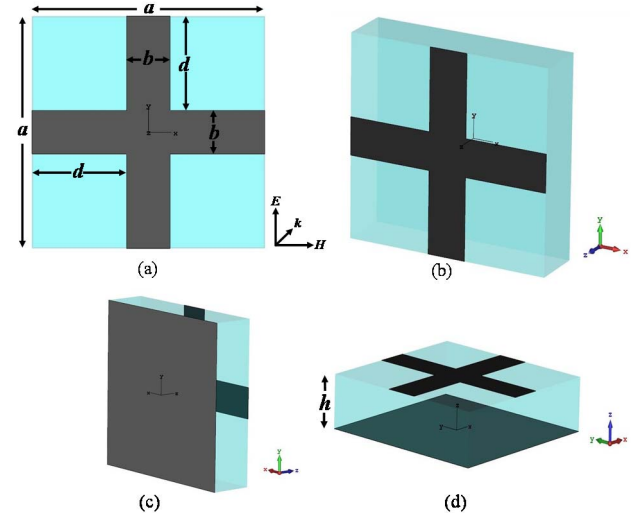


**Fig. 1.** (a) Top view, (b) perspective view, (c) back view and (d) side view of the proposed structure ( $a = 8 \mu\text{m}$ ,  $b = 3.25 \mu\text{m}$ ,  $d = 1.5 \mu\text{m}$ ,  $h = 2 \mu\text{m}$ ).

On the top surface of the unit cell a plus-shaped graphene pattern is grown on a 2  $\mu\text{m}$  thick amorphous  $\text{SiO}_2$  with dielectric constant of 3.9 and a loss tangent of 0.0006. The other side of the  $\text{SiO}_2$  is covered completely with graphene. The thickness of the graphene sheet is taken as 1 nm. The top view, perspective view, back view and side view of the proposed 3D geometry of the unit cell are picturized in Fig. 1(a), Fig. 1(b), Fig. 1(c) and Fig. 1(d) in accordance. The top graphene geometry is optimized through several developments so that it can achieve wide absorption bandwidth in the previously said spectral range that is called mid infrared range (MIR). The structural dimensions of the design are mentioned at the caption of Fig. 1. The top graphene layer is acting as a matching circuit with impedance as similar to the free space impedance ( $377 \Omega$ ). The overall geometry is called a metasurface as its dimensions are in the sub-wavelength region of the order

of  $\lambda/7.5$  and the EM wave can easily enter into it without diffraction or scattering. The bottom graphene layer is acting as a reflector, which ensures no transmission of EM wave due to its semi-metallic property. The set-up of the structure is organized in such a way that EM wave first enters through the top graphene layer into the structure and then it encounters multiple reflections where the whole structure acts as a Fabry-Perot cavity [10]. This multiple reflection loss creates maximum absorption within the whole structure. The directions of electric field ( $E$ ), magnetic field ( $H$ ) and propagation vector ( $k$ ) are also shown in Fig. 1(a).

### 3. Simulation and Results

In this article, one single unit cell is designed and analysed elaborately. The whole structure is an infinite periodic array of the aforesaid unit cell described in Fig. 1. The design is simulated in CST Microwave Studio under periodic boundary condition using frequency domain solver. The calculated reflectivity ( $R$ ), transmittivity ( $T$ ) and corresponding absorptivity ( $A$ ) responses are inked on Fig. 2(a) and Fig. 2(b) systematically. The simultaneous minimization of both  $R$  and  $T$  of the EM wave within the structure confirms occurrence of absorption within the same. The structure is unique in nature to exhibit more than 90% absorptivity from 7 THz to 19 THz specifically within the wide absorption bandwidth. This is illustrated from the Fig. 2(b) clearly.

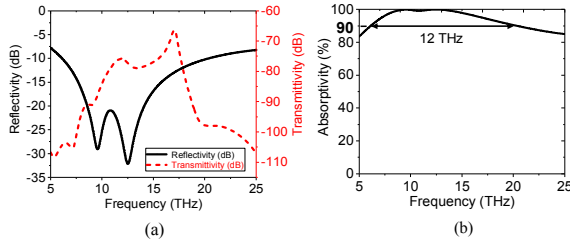


**Fig. 2.** Responses of (a) reflectivity (dB) and (b) absorptivity (%) of the structure whose unit cell is shown in Fig. 1.

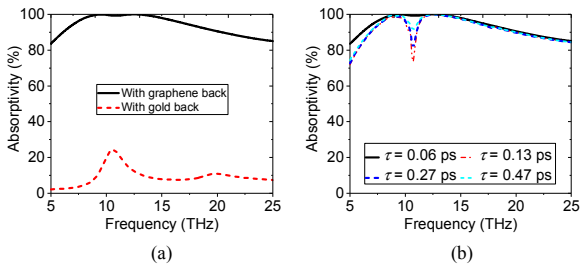


**Fig. 3.** Absorptivity response under the control of (a) comparative study of gold and graphene bottom layer and (b) relaxation time ( $\tau$ ).

The bottom reflector is examined with gold metal and semi-metal graphene to check the performance of both and the comparative absorptivity responses are graphed together in Fig. 3(a). It is observed that wideband absorption can be achieved using bottom graphene layer. In terahertz region graphene exhibits distinctive high conductivity [16]. It has two types of conductivities, viz.,

interband conductivity and intraband conductivity. The intraband conductivity is more influential than the interband one in the lower terahertz region [11]. The interband conductivity is developed with the assumption of  $k_B T < |\mu|, \hbar\omega$  and can be neglected due to Pauli's blocking principle [12]. The conductivity of the extremely thin 2D graphene sheet can be computed using Kubo's formula [11].

The absorptivity response has its several forms due to the variety of changes made in the structural dimensions and parametric changes in graphene sheet of the proposed 3D geometry. First, the parameters of the graphene layers are changed. The relaxation time ( $\tau$ ) of the graphene layer defines the duration between two consecutive collisions of the electrons on the graphene layers. The performance of the proposed metasurface structure has been studied for different  $\tau$  where the best response is reached for  $\tau = 0.06$  ps as shown in Fig. 3(b). Another important parameter pertinent to graphene layer is the chemical potential ( $\mu_c$ ) which plays an important role in the absorptivity response. Actually, variation in  $\mu_c$  provides tunability in conductivity of the graphene sheet [13] which leads to the tunable characteristics in the absorption bandwidth [14]. Changes in  $\mu_c$  are done on both the top layer and the bottom layer graphene patterns but single at a time. The corresponding absorptivity responses regarding the above fact are shown in Fig. 4(a) and Fig. 4(b) respectively. The top layer chemical potential is denoted by  $T\mu$  and the bottom layer

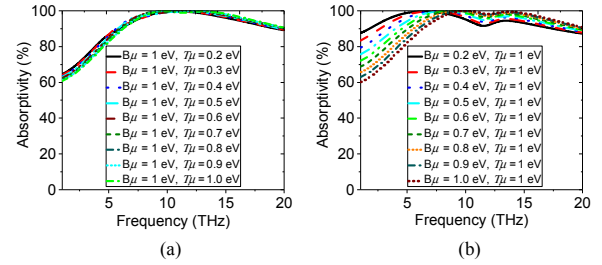


**Fig. 4.** Absorptivity response under the control of (a) top layer chemical potential ( $T\mu$ ) and (b) bottom layer chemical potential ( $B\mu$ ).

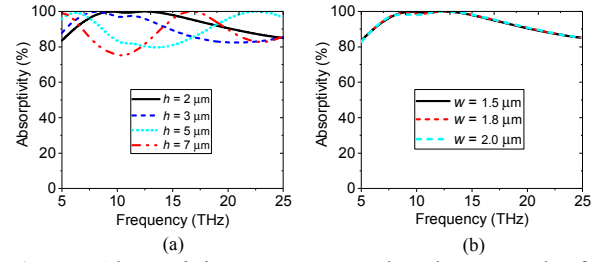


**Fig. 5.** Absorptivity response under the control of (a) substrate thickness ( $h$ ) and (b) width of the arms variation ( $w$ ).

chemical potential is expressed as  $B\mu$ . The best performance is achieved when  $B\mu = 0.2$  eV and  $T\mu = 1$  eV and it can be evident from Fig. 4(b).

The structural dimensions are nurtured to check the absorptivity responses further. The variations in substrate height generates different absorptivity responses and they are captured in Fig. 5(a). The changes in absorption occur due to the changes in coupling strength between the top

layer and the bottom layer. Next, the width of the top layer plus-shaped graphene arms is altered. This modification has not much significant changes in absorptivity performance and it can be verified from Fig. 5(b). Moreover, the surface current distribution patterns are presented here at two different frequencies to validate the magnetic excitation and electric excitation. For that, the authors have checked the surface current distributions vectors of the top layer and bottom layer of the overall package. In the first case, at 9.55 THz, the top layer and the bottom layer surface current distribution vectors are anti-parallel which leads to magnetic excitation depicted in Fig. 6(a). In the second case, at 12.5 THz, the top layer and the bottom layer surface current distribution vectors are parallel to each other which creates electric excitation shown in Fig. 6(b).

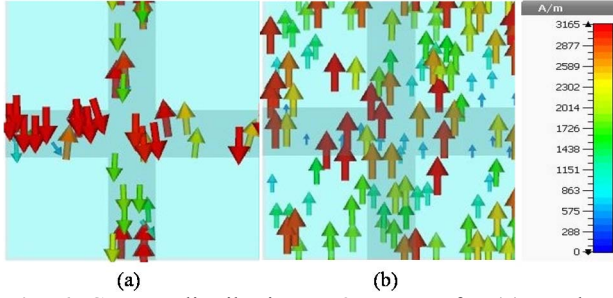


**Fig. 6.** Current distribution at 9.55 THz for (a) top layer and (b) bottom layer

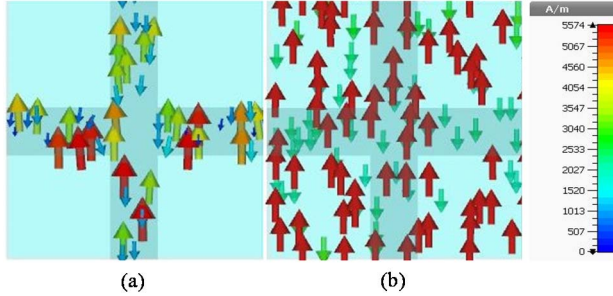


**Fig. 7.** Current distribution at 12.50 THz for (a) top layer and (b) bottom layer

#### 4. Response Under Polarization Angle and Oblique Incidences

The designed prototype has been examined under different situations to have a check on absorptivity response. The EM wave has its different polarization states changing with respect to time. The above said concept can be realized using the set-up described in Fig. 8(a) when the EM wave is incident upon the top surface of the structure normally ( $\theta = 0^\circ$ ). The corresponding absorptivity response is shown in Fig. 8(b). The performance is invariant upto  $45^\circ$  of the polarization angle and this fact is a validation of polarization insensitivity of the designed model as it has four-fold symmetry.

The structure has also been examined under different incident angles ( $\theta$ ) for both transverse electric (TE) and transverse magnetic (TM) polarizations. The frameworks for oblique incidence of the EM wave under both TE and TM polarizations are shown in Fig. 9(a) and Fig. 10(a). The corresponding responses of absorptivity are presented in

Fig. 9(b) and Fig. 10 (b) respectively where the bandwidth enhanced absorption upto  $60^\circ$  incident angles is realized.

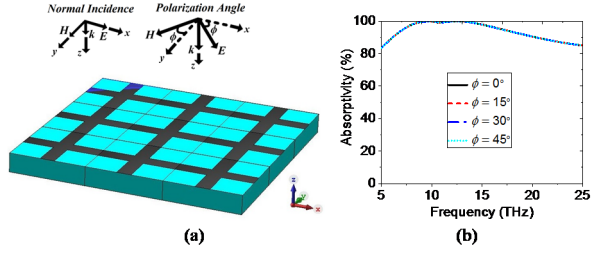


**Fig. 8.** (a) Framework of the overall structure under polarization angle variation with (b) absorptivity response ( $\phi$ : angle of polarization).

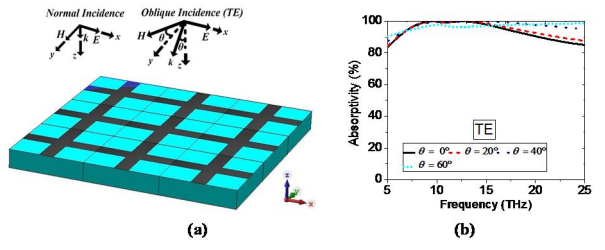


**Fig. 9.** (a) Framework of the structure under oblique incidence variation with (b) absorptivity response ( $\theta$ : angle of incidence).

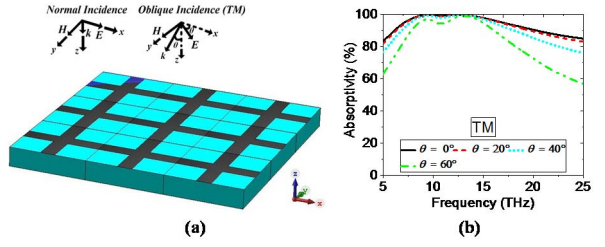


**Fig. 10.** Absorptivity response of the overall structure under (a) TE polarization and (b) TM polarization.

**Table I.** Comparison with existing graphene-based absorber

| Grafe<br>ne based<br>absorbe<br>rs | Fraction<br>al<br>Bandwid<br>th | Frequen<br>cy region | Thickne<br>ss    | Perio<br>d of<br>unit<br>cell |
|------------------------------------|---------------------------------|----------------------|------------------|-------------------------------|
| Chen <i>et.<br/>al</i> [9]         | 30 %                            | 8.5-11.5<br>THz      | $\sim\lambda/2$  | $\sim\lambda/2$               |
| Fu <i>et. al.</i><br>[15]          | 28.26 %                         | 5.5-9.5<br>THz       | $\sim\lambda/5$  | $\sim\lambda/11$              |
| Huang<br><i>et. al.</i><br>[16]    | 13.37 %                         | 1-1.8<br>THz         | $\sim\lambda/14$ | $\sim 3\lambda/4$             |
| Xu <i>et. al</i><br>[17]           | 80 %                            | 1.5-3.5<br>THz       | $\sim\lambda/6$  | $\sim\lambda/20$              |
| Proposed<br>Design                 | 90 %                            | 7-19 THz             | $\sim\lambda/30$ | $\sim\lambda/7.5$             |

This particular design has some advantages over the existing graphene-based absorbers tabulated in Table I. It is observed from Table I that the proposed structure offers improved performance with ultrathin characteristics.

## 7. Conclusion

A distinctive metasurface-based absorber with polarization insensitivity has been presented in this literature. It has achieved a broad absorption bandwidth of 12 THz from 7 THz to 19 THz with more than 90% absorptivity. The designed prototype works fine upto 60° of the incidence angle of the EM wave for both TE and TM polarizations. The absorber is ultra-thin in nature with the thickness of approximately  $\lambda/30$ . The periodicity of the design is also in the order of  $\lambda/7.5$ . This absorber can be very promising for the ‘Terahertz Gap’ applications for 5G communications and beyond.

## 8. Acknowledgements

SB and SD acknowledge SERB, Govt. of India for providing early career research grants for this work.

## 9. References

- [1] C. Fang, J. S. Gao, and H. Liu, “A novel metamaterial filter with stable passband performance based on frequency selective surface,” *AIP Advances*, **4**, 11, July 2014, pp. 077114, doi:10.1063/1.4890108.
- [2] K. Saurav, D. Sarkar and K. V. Srivastava, "CRLH Unit-Cell Loaded Multi-Band Printed Dipole Antenna," *IEEE Antennas and Wireless Propagation Letters* **13**, 29 April 2014, pp. 852-855, doi:10.1109/LAWP.2014.2320918.
- [3] D. Schurig, J.J. Mock, B.J. Justice, S.A. Cummer, J.B. Pendry, A.F. Starr, D.R. Smith, “Metamaterial electromagnetic cloak at microwave frequencies,” *Science* **314** 10 November 2006, pp. 977–980, doi: 10.1126/science.1133628.
- [4] J. G.-Garcia, F. Martin, F. Falcone, J. Bonache, I Gil, T. Lopetegi, M. AG Laso, M. Sorolla, and R. Marques, “Spurious passband suppression in microstrip coupled line band pass filters by means of split ring resonators,” *IEEE Microwave and Wireless Components Letters*, **14**, 24. August 2004, pp. 416-418, doi:10.1109/LMWC.2004.832066.
- [5] S. Bhattacharyya, S. Ghosh and K. V. Srivastava, “A wideband cross polarization conversion using metasurface,” *Radio Science Journal*, **52**, 03, November 2017 pp. 1395-1404, doi:10.1002/2017RS006396.
- [6] Q. Y. Wen, H. W. Zhang, Y. S. Xie, Q. H. Yang and Y. Li. Liu, “Dual-band terahertz metamaterial absorber : Design, fabrication and characterization,” *Applied Physcis Letters*, **95**, 18, December 2009, pp. 241111, doi:10.1063/1.3276072.
- [7] S. Ghosh, S. Bhattacharyya, and K. V. Srivastava, “Bandwidth enhancement of an ultrathin polarization insensitive metamaterial absorber,” *Microwave and Optical Technology Letters*, **56**, 23, December 2013, pp. 350-355, doi: 10.1002/mop.28122.
- [8] S. Bhattacharyya, and K. V. Srivastava, “Tripple band polarization independent ultra-thin metamaterial absorber using ELC resonator,” *Journal of Applied Physics*, **115**, 13, February 2014, pp. 064508, doi: 10.1063/1.4865273.
- [9] D. Chen, J. Yang, J. Zhang, J. Huang and Z. Zhang, “Tunable broadband terahertz absorbers based on multiple layers of graphene ribbons,” *Scientific Reports*, **7**, 20, November 2017, pp. 15836(1-8), doi: 10.1038/s41598-017-16220-9.
- [10] J. Grant, Y. Ma, S. Saha, L. B. Lok, A. Khalid and D. R. S. Cumming, “Polarization insensitive terahertz metamaterial absorber,” *Optics Letters*, **36**, 15, April 2011, pp. 1524, doi:10.1364/OL.36.001524.
- [11] R. Bala, A. Marwaha, and S. Marwaha, “Mathematical formulation of surface conductivity for graphene material,” *Journal of Engg. Sci. & Tech.*, **12**, 01, January 2017, pp. 1677-1684, doi: 10.11591/telkomnika.v16i3.8307.
- [12] N. Kakenov, O. Balci, E. O. Polat, H. Altan and C. Kocabas, “Broadband terahertz modulators using self-gated graphene capacitors,” *Journal of the Optical Society of America B*, **32**, 01, September 2015, pp. 1861, doi:10.1364/JOSAB.32.001861.
- [13] X. Huang, X. Zhang, Z. Hu, M. Aqeeli, A. Alburaiyan, “Design of broadband and tunable terahertz absorbers based on graphene metasurface: equivalent circuitmodel approach,” *IET Microw. Antennas Propag.*, **9**, 19, March 2015, pp. 307-312, doi: 10.1049/iet-map.2014.0152.
- [14] H. Nasari, M. S. Abrishamian, “Electrically tunable, plasmon resonance enhanced, terahertz third harmonic generation,” *RSC Advances*, **6**, 23, May 2016, pp. 50190-50200, doi:10.1039/C6RA08086C.
- [15] P. Fu, F. Liu, G. J. Ren, F. Su, D. Li, and J. Q. Yao, “A broadband metamaterial absorber based on multi-layer graphene in the terahertz region,” *Optics Communications*, **417**, 15, June 2018, pp. 62-66, doi: 10.1016/j.optcom.2018.02.034.
- [16] H. Huang, H. Xia, W. Xie, Z. Guo, H. Li and D. Xie, “Design of broadband graphene metamaterial absorbers for permittivity sensing at mid-infrared regions,” *Scientific Reports*, **8**, 08, March 2018, pp. 4183, doi:10.1038/s41598-018-22536-x.
- [17] B. Z. Xu, C. Q. Gu, Z. Li, L. L. Liu, and Z. Y. Niu, “Circuit model for graphene based absorber at low terahertz frequencies,” *Journal of Physics D*, **47**, 30, May 2014, pp. 255013, doi: 10.1088/0022-3727/47/25/255103.